PHOTOELASTICITY

José L.F. Freire
Mechanical Engineering Department, Catholic University of Rio de Janeiro

Arkady Voloshin
Department of Mechanical Engineering and Mechanics, Lehigh University

Key Words: photoelasticity, stress, strain, experimental stress analysis, birefringence

Contents

Summary

Photomechanics entails experimental techniques that use properties of light propagating through loaded or deformed components to determine and analyze the relative displacements in the material in order to establish their strain and stress fields. Photoelasticity is a branch of Photomechanics. It employs models constructed from materials transparent to the light being used. These materials display birefringence under applied stress and are observed under polarized light using an instrument called a polariscope. The photoelastic response consists of two families of fringes – isochromatic and isoclinic – which are observed in the polariscope.

Photoelasticity may be applied to models in the laboratory or to prototypes in the field,

as well as to 2D or 3D studies. Thus, it is a whole field technique. Although the optical response shows stress distributions over a relatively large spatial dimension, it nevertheless allows for an accurate determination of stress states in localized areas or at specific points of a component. Consequently, photoelasticity indicates not only the most loaded areas of the observed component, but can also provide accurate stress values at any critical point.

1. Introduction

The area of Photomechanics entails experimental techniques that use properties of light propagating through loaded or deformed components to determine and analyze relative displacements in the material in order to establish their strain and stress fields.

Photoelasticity is a branch of Photomechanics. It employs models constructed from materials transparent to the light being used. These materials exhibit birefringence under applied stress and are observed under polarized light using an instrument called a polariscope.

Photoelasticity may be applied to models in the laboratory or to prototypes in the field. Thus, it is a whole field technique. Although the optical response shows stress distributions over a relatively large spatial dimension, it nevertheless allows for an accurate determination of stress states in localized areas or at specific points of a component. Consequently, photoelasticity indicates not only the most loaded areas of the observed component, but can also provide accurate stress values at any critical point. Photoelasticity may be applied to 2D or to 3D studies and can be extended to non-linear elastic, elastic-plastic and dynamic problems as well. In these cases the techniques are most appropriately called Non-linear Photomechanics, Photoplasticity and Photodynamics.

A few examples of photoelasticity are shown below. Figure 1a shows the localized photoelastic response used to determine the stress concentration factor of a sharp U-notch. Figure 2b shows the whole field response of a C-shaped model loaded by compressive forces. Qualitative observation of the optical response allows the identification of the areas under the most stress, which may be inspected quantitatively under higher magnification or by using some other experimental technique. Figure 1c shows residual fringes caused by the fabrication process of incandescent light bulbs. In this case photoelasticity is used as an inspection tool in the production of glassware.

The photoelastic response consists of two families of characteristic lines that are observed in the polariscope: isochromatic and isoclinic fringes. The isochromatic fringes correspond to the geometric locus of material points that present the same principal stress differences. The stress-optic law (1) relates the principal stress differences $\sigma_{\mathrm{I}} - \sigma_{\mathrm{II}}$ with the measured isochromatic fringe order N, where t is the thickness of the model at the point under analysis and f_σ is the stress fringe value that depends on the photoelastic material and the wave length of the light used in the observation.

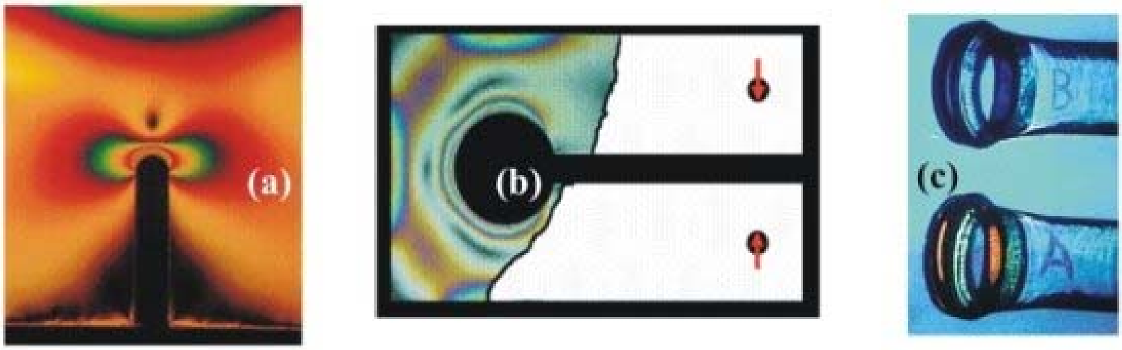

Figure 1. Examples of photoelasticity. (a) stress concentration area of a sharp U-notch, (b) whole field stress distribution image of a C-shaped model, (c) residual stresses in light bulbs caused by the fabrication process.

$$\sigma_{\mathrm{I}} - \sigma_{\mathrm{II}} = \frac{N}{t} f_{\sigma} \tag{1}$$

The isoclinic fringes correspond to the geometric locations of the observed material points which make 0^{o} or 90^{o} with the polariscope axes.

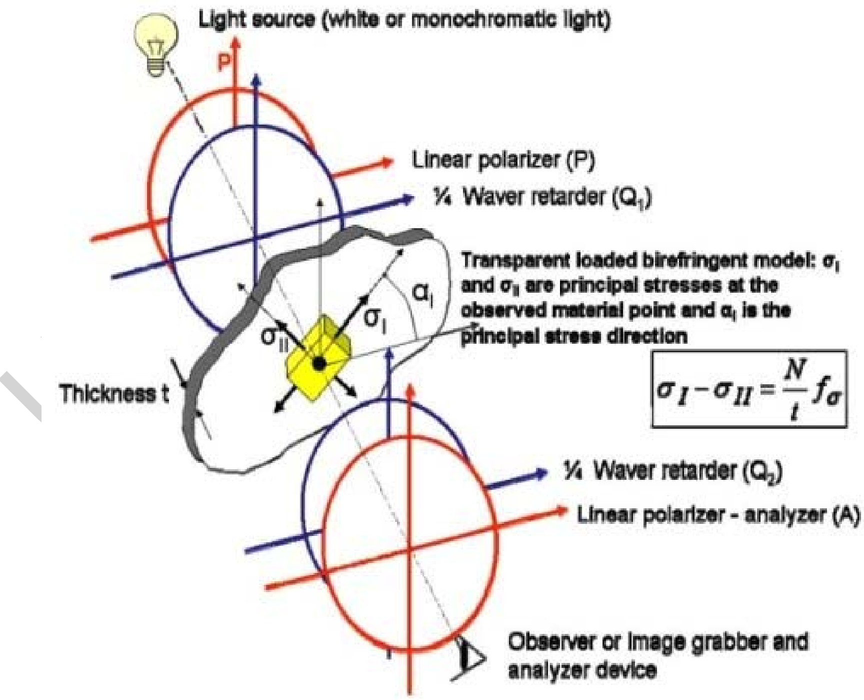

Figure 2. A loaded model inserted into the working field of a light transmission polariscope consisting of a light source, two linear polarizers, two wave retarders and an observer.

The polariscope is the basic instrument used in the photoelastic experiment. Essentially, it consists of a light source, two plates of linear polarizers and two plates of wave retarders. Besides other possible arrangements, polariscopes are generally employed in one of two configurations: the plane polariscope, which uses linear or plane polarized light and shows the families of isochromatic and isoclinic fringes; the circular polariscopes, which uses circularly polarized light to show the family of isochromatic fringes. A sketch of a polariscope that involves a loaded model is presented in Figure 2.

Usually, the plane polariscope uses the linear polarizers in a crossed arrangement. A common arrangement of the circular polariscope also uses crossed wave retarders. The polariscope depicted in Figure 2 works in a plane polariscope mode since the principal axes of wave retarders were placed parallel to the axes of the linear polarizers in order to be ineffective.

2. Light

The electromagnetic theory of light propagation is used to explain the photoelastic effect adequately. The wave Eq. (is presented in Eq. ((2). The solution of the wave Eq. (is the space of harmonic functions. These functions can be represented by a series combination of sine functions with arguments given by multiples of the basic frequency w (rd/s) or f (Hertz).

If white light is used, all visible wave lengths λ will make up the harmonic function. If only one wave length is used (monochromatic light), the solution of the unidirectional wave Eq. ((3) with light propagating in the positive direction is given by Eq. ((4). In this last equation, E is the propagating light vector, which is parallel to a given plane; its amplitude is given by E_0. Vector E can be seen as the sum of two orthogonal vectors that propagate in the planes x and y.

$$\nabla^2 E = \frac{1}{c^2}\frac{\partial^2 E}{\partial t^2} \tag{2}$$

$$\frac{\partial^2 E}{\partial z^2} = \frac{1}{c^2}\frac{\partial^2 E}{\partial t^2} \tag{3}$$

$$E = E_o \cos(wt + \phi) \qquad w = 2\pi f \qquad T = \frac{1}{f} \qquad \lambda = T.c \tag{4}$$

3. Linear Polarizers

Light generated at a diffuse light source propagates in all possible directions. For each direction the electrical vectors have components in all possible planes. Figure 3 shows light propagating in a specific direction and passing through a polarizer filter. After crossing the polarizer the light wave will be represented by the components of the electrical vector that propagates parallel to the plane of the filter’s polarization.

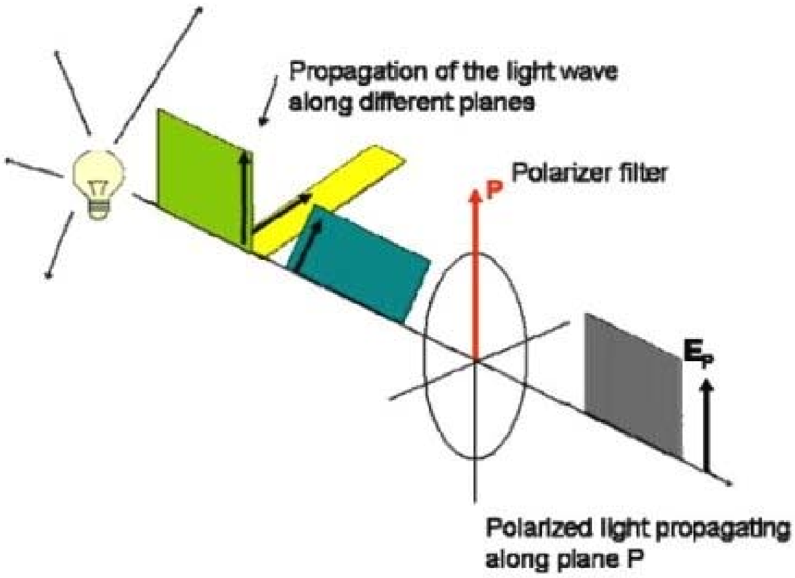

Figure 3. Propagation of light across a plane polarizer filter

When light propagates parallel to a given plane it is called plane or linearly polarized light. Light may be linearly polarized by being reflected from a flat surface if an adequate angle of incidence is chosen for the incident light ray. Equation (5) and Figure 4 depict the E_{0^o} (parallel) E_{90^o} (orthogonal) components of the incident and reflected light rays that strike a reflective surface. Equation (5) shows that the reflected and incident light intensities I_r and I_i are related by the reflection coefficient R, which is different for the parallel and orthogonal waves. For the air-glass media interface there is a critical angle $\alpha_p = 57^o$ such that the reflected component E_{ry} is zero. Figure 4 illustrates this phenomenon.

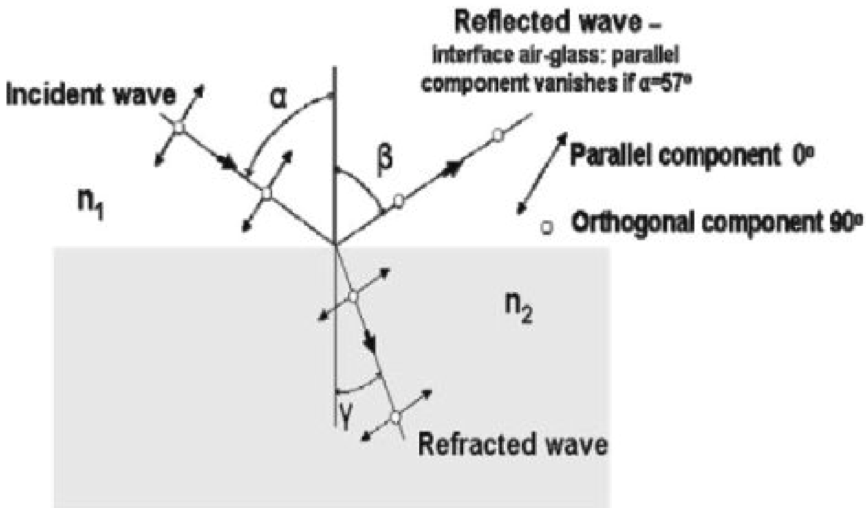

Figure 4. Incident, reflective and refracted waves

$$I_{\mathrm{r}} = R.I_{\mathrm{i}}$$
$$R_{0^{\mathrm{o}}} = \frac{\tan^2(\alpha-\gamma)}{\tan^2(\alpha+\gamma)} \qquad R_{90^{\mathrm{o}}} = \frac{\sin^2(\alpha-\gamma)}{\sin^2(\alpha+\gamma)} \tag{5}$$
$$\frac{\sin\alpha}{\sin\gamma} = \frac{n_2}{n_1}$$

Another way of generating large fields of view of polarized light is accomplished by at first using a transparent plastic sheet of polyvinyl alcohol saturated with iodine. The necessary orientation of the molecules is achieved by stretching (for example, sheets fabricated by Polaroid Inc. as types HN22, HN32 and HN38), as is shown in Figure 5. The filter classified as HN22 is the most appropriate for use in photoelasticity.

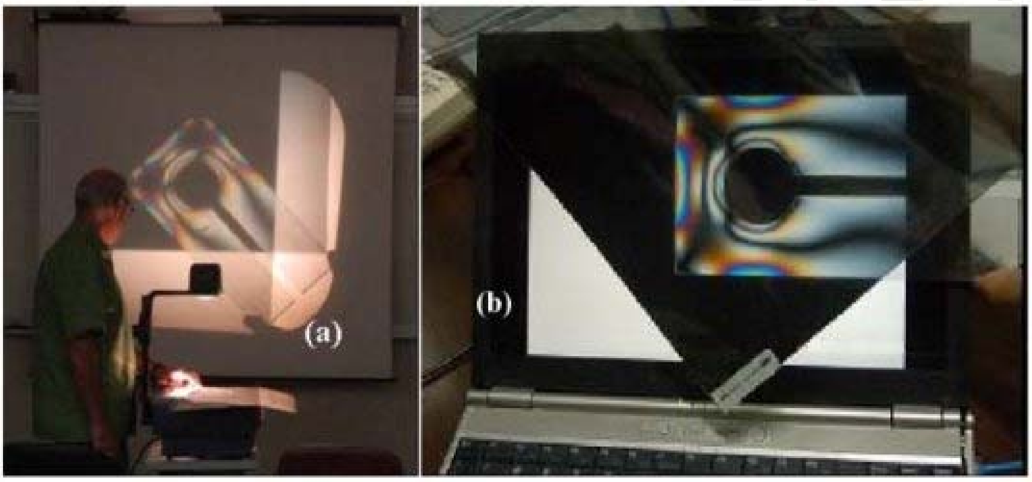

Figure 5. Polarizer filters used in a demonstration of photoelasticity: (a) an overhead projector is used as the light source. Polarizer filters are superposed with axes crossed. A loaded C model is placed between the filters; (b) a laptop screen, which emits linearly polarized light, is used together with a polarizer filter to show an arrangement of a plane polariscope and isochromatic and isoclinic fringes generated in a loaded C-shaped model.

4. Wave Plate

The wave plate transmits the components of the light through two orthogonal planes called F (fast) and S (slow). The components E_{F} and E_{S} of light vector E cross the filter thickness at different velocities, causing a relative retardation between E_{F} and E_{S} and consequently an elliptic propagation of the light after emerging from the filter. This behavior is depicted in Figure 6, where the relative linear retardation δ (or angular retardation $\Delta = 2\pi\delta / \lambda$) is schematically shown between components E_{F} and E_{S}.

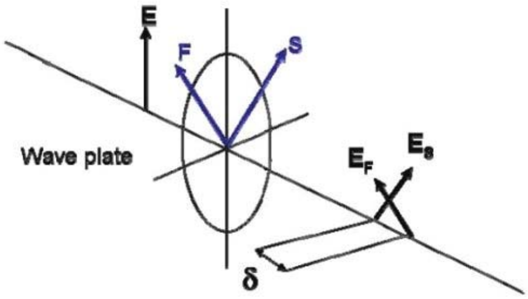

Figure 6. Light crossing a wave plate where F and S are, respectively, the fast and the slow directions of propagation of the electrical light vector.

Equations (6a) and (6b), respectively, establish the conditions for the resulting elliptic light propagated as either circular or a linear polarized light.

Circular polarized light if: $\begin{cases} \delta = \dfrac{\lambda}{4} \\ E_F = E_S \end{cases}$ (6a)

Linear or plane polarized light if: $\delta = 0$ (6b)

A wave plate with a phase shift of $\pi / 2$ is often used in photoelasticity and is called a *quarter-wave* plate.

5. Plane Polariscope

The plane polariscope consists of a light source and two linear polarizer plates, which are usually employed with their polarization axes crossed (Figure 7). The light intensity I perceived by the observer is zero if there is no stressed model in the working field. The plane polariscope is used for observing isochromatic and isoclinic fringes.

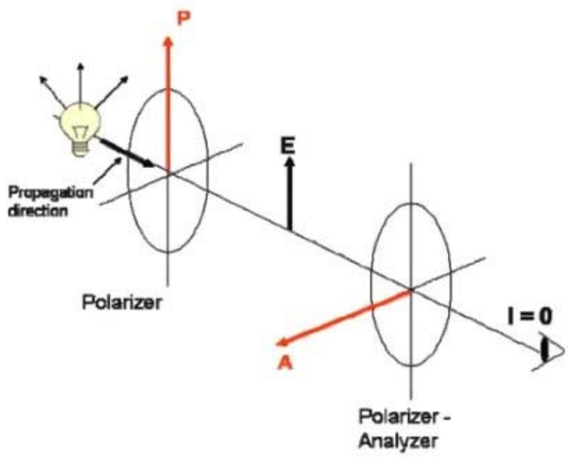

Figure 7. Plane polariscope with crossed polarizer plates.

6. Circular Polariscope

The circular polariscope is used for observing isochromatic fringe orders. The name 'circular' comes from the fact that it uses circular propagating light in its working field (Figure 8). The light wave is generated in the light source and crosses the polarizer plate to be plane polarized. A ¼ wave plate is placed with its fast and slow axes making a 45^o angle to the polarizer. This angle enables both amplitudes E_S and E_F to become equal. The second wave plate is arranged to be crossed to the first one. This arrangement regenerates the initial plane of polarization. The observer does not perceive light intensity in this arrangement unless a loaded birefringent model is positioned in the working field. The zero light intensity is caused by the placement of an analyzer with axes crossed to the first polarizer. Other arrangements of axes of polarizers and wave plates are possible and are used in some applications.

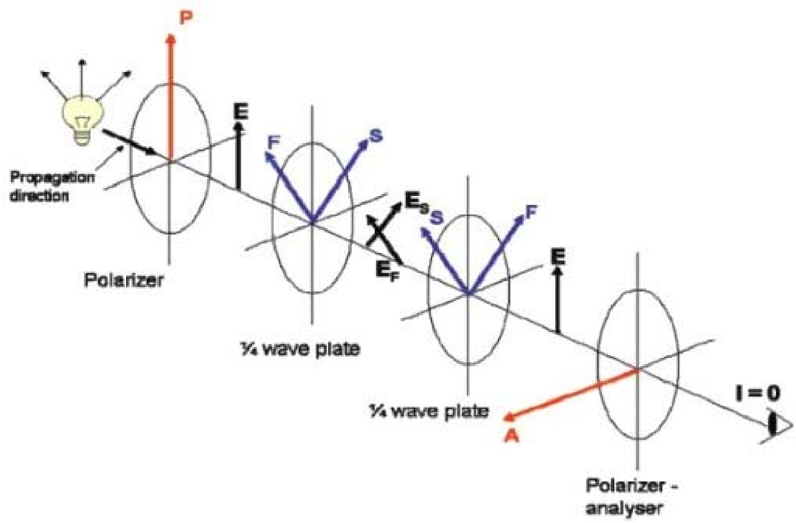

Figure 8. Circular polariscope in a crossed-crossed arrangement

7. Model of Birefringent Material

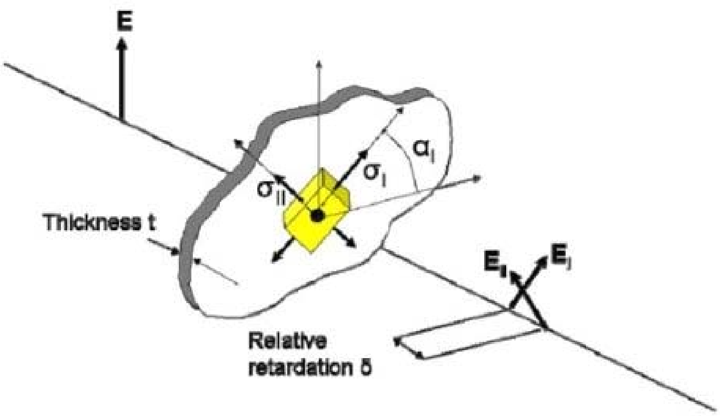

Figure 9. Effect of the state of stress at a point in a loaded model of birefringent material on incident light vector E.

Photoelastic models are built from birefringent materials. These materials behave as ordinary general wave plates. They cause retardation between the components of the light vector that passes through the deformed material. The relationship between incident light vector E and the state of stress in the observed point of a sample of birefringent material is illustrated in Figure 9.

The stress state causes retardation δ between the components of the electrical light vector that are parallel to the principal directions of stress (defined by angle α).

The relative retardation δ caused by the stress state depends on the principal stress difference $\sigma_{\mathrm{I}} - \sigma_{\mathrm{II}}$, the thickness of the component being observed t, the wave length λ of the incident light and the birefringence constant of the material, K (Eq. (7)). The stress fringe value f_σ and the strain fringe value f_ε are also used and their relationship is defined by the material elastic constants - the Young modulus E and the Poisson coefficient μ (Eq. (8)).

$$\sigma_{\mathrm{I}} - \sigma_{\mathrm{II}} = \frac{\delta}{t} K = \frac{\delta}{t.\lambda} f_\sigma = \frac{N}{t} f_\sigma = \frac{\Delta}{2\pi.t} f_\sigma \qquad (7)$$

$$\varepsilon_I - \varepsilon_{II} = \frac{N}{t} f_\varepsilon \qquad f_\varepsilon = \frac{1+\mu}{E} f_\sigma \qquad (8)$$

8. Loaded Model in a Plane Polariscope

Figure 10 shows a loaded model (disk under a diametrical compression) in the working field of a plane polariscope. The intensity of light perceived by an observer or image grabber device is proportional to the square of the amplitude of the electrical vector that passes through the analyzer. Light intensity is given by Eq. (9 (see the development in section 10 - Jones Calculus). The black fringes (zero light intensity) observed in the whole field image of the model are the isochromatic and the isoclinic fringe families.

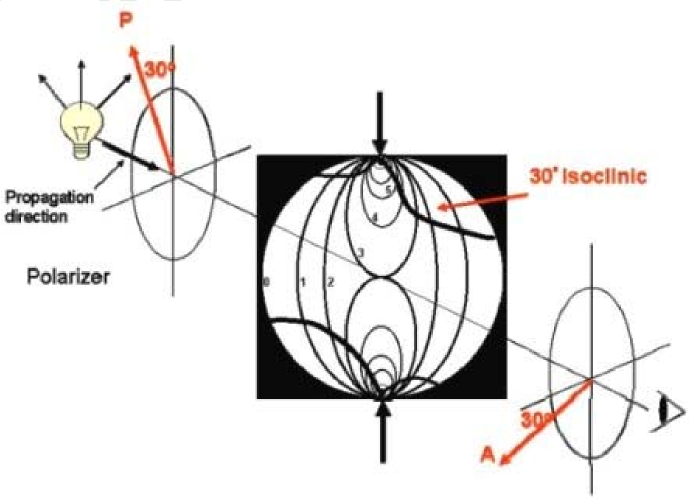

Figure 10. Loaded model (disk under diametrical compression) in a plane polariscope

$$I \propto E_a^2 \propto E_o^2 .\sin^2 2\alpha .\sin^2 \frac{\Delta}{2} \tag{9}$$

Light intensity will be zero when:

$$I = 0 \quad \text{if :} \quad \sin^2 2\alpha = 0 \quad \Leftrightarrow \quad \alpha = 0, \frac{\pi}{2} \tag{10}$$

or

$$I = 0 \quad \text{if :} \quad \sin^2 \frac{\Delta}{2} = 0 \quad \Leftrightarrow \quad \Delta = 0, 2\pi, 4\pi, \ldots \tag{11}$$

The geometric loci of such fringes are the isochromatic and isoclinic fringes. These fringes are shown and numbered in Figure 11. It can be seen that the isoclinic fringes are the loci of all points whose principal stress directions coincide with the polariscope axes, forming angles of $\alpha = 0^o$ or 90^o. Figure 10 shows material points whose principal stress directions form a 30^o angle with the original polariscope axes. In order to observe these points with light intensity zero, the model or the polariscope must be rotated at an angle equal to 30^o. The points where light intensities become zero in this position define the 30^o isoclinic.

The isochromatic fringe orders *N* are defined by the ratio of relative retardation and wavelength δ/λ or $\Delta/2\pi$. Equation (11) shows that whenever retardation corresponds to a full wavelength, the light intensity becomes zero. Full fringe orders are multiples of the light wavelength. They are numbered in Figure 11 for the diametrically compressed disk. Finding full or partial fringe orders and differentiating isoclinics from isochromatic fringes are the job of a photoelastician.

-
-
-

Bibliography

1. Durelli, A.J. e Riley W.F. (1965). *Introduction to Photomechanics*, Prentice-Hall, Englewood Cliffs, NJ. [Classical book in the field of Photoelasticity]

2. Dally, J.W. e Riley, W.F. (2005). *Experimental Stress Analysis*, McGraw-Hill, 4th ed. [classical book in the field of Experimental Sress Analysis – two chapters in Photoelasticity]

3. Jessop, H.T. E Harris, F.C. (1950). *Photoelasticity: Principles and Methods*, Dover Publications, NY. [Classical book in the field of Photoelasticity]

4. Kuske, A. E Robertson, G. (1974). *Photoelastic Stress Analysis*, John Wiley & Sons, NY. [Classical book in the field of Photoelasticity]

5. Frocht, M.M. (1941). *Photoelasticity*, John Wiley & Sons, NY, vol.1. [Classical book in the field of Photoelasticity]

6. Frocht, M.M. (1948). *Photoelasticity*, John Wiley & Sons, NY, vol.2. [Classical book in the field of Photoelasticity]

7. Ramesh, K. (2000). *Digital Photoelasticity*, Springer. [Classical book in the field of modern and digital Photoelasticity]

8. Doyle, J.F. (2004). *Modern Experimental Stress Analysis*, John Wiley & Sons. [Modern approach to experimental stress analysis where photoelasticity is included]

9. Burger, C.P. (1993). *Photoelasticity*, Chapter 5 of Handbook of Experimental Mechanics, ed. by A.S. Kobayashi, Soc. Experimental Mechanics and VCH publishers, New York, pp.162–281.

10. Aben, H., Guillemet, C. (1993). *Photoelasticity of Glass*, Springer, Berlin.[Reference in photoelasticity applied to glass]

11. Srinath, L.S. (1983). *Scattered Light Photoelasticity*, Tata McGraw-Hill, New Delhi. .[Reference in scattered light photoelasticity]

12. Cernosek, J. (1980). Three-dimensional photoelasticity by stress freezing, *Experimental Mechanics*, 20(12), 417–426.[Deals with analysis of slices in 3D photoelasticity]

13. Dally, J.W. (1980). An introduction to dynamic photoelasticity, *Experimental Mechanics*. 20 409-416. [Reference in dynamic photoelasticity]

14. Aben, H. (1979). *Integrated Photoelasticity*, McGraw-Hill, New York. [Reference in complex propagation of light in photoelasticity]

15. Javornicky, J. (1974). *Photoplasticity*, Elsevier Scientific Publishing Company, New York.[Useful approach of photoplasticity]

16. Heywood, R.B. (1952). *Designing by Photoelasticity*, Chapman and Hall Ltd., London.[[reference in applied photoelasticity]

17. Voloshin, A., Burge, C.P. (1983). Half fringe photoelasticity – a new approach to whole field stress analysis, *Experimental Mechanics*, 23(9), 304–314.[One of the precursors in modern digital photoelasticity]

18. Sanford, R.J. (1980). Application of the least squares method to photoelastic analysis, *Experimental Mechanics*. 20, 192–197. [Useful in refining photoelastic data with application to fracture mechanics].

19. Zandman, F., Redner, S., Dally, J.W. (1977). *Photoelastic Coatings*, Soc. Experimental Stress Analysis Monograph No.3, Soc. Experimental Stress Analysis, Bethel, CT. [Reference in birefringent coating photoelasticity]

20. Dally, J.W., Prabhakaran, R. (1971). Photo-orthotropic elasticity, *Experimental Mechanics*, 11, 346–356. [Reference in anisotropic photoelasticity]

21. Sanford, R.J. (1986). On the range and accuracy of spectrally scanned white light photoelasticity, Proc. SEM Spring Conference on Experimental Mechanics, Los Angeles, Soc. Experimental Mechanics, Bethel, CT, 901–908. [Reference and precursor in modern automated photoelasticity]

22. Ajovalasit, A., Barone, S., Petrucci, G. (1995). Towards RGB photoelasticity: full-field automated photoelasticity in white light, *Experimental Mechanics*, 35(3), 193–200. [Classical reference in digital RGB photoelasticity]

23. Lesniak, J.R., Bazile, D.J., Zickel, M.J. (1999). New coating techniques in Photoelasticity. SEM Spring Conference on Experimental Mechanics, Society for Experimental Mechanics, Bethel, CT. [Reference in automated birefringent coating photoelasticity]

24. Cloud, G. (2008). Part 30: Photoelasticity II- Birefringence in materials, Optical Methods in Experimental Mechanics - Series Back to Basics, *Experimental Techniques*, 32, 1, 13-16. [Example of one of a series of articles focused on education in experimental mechanics. This and other articles deal with photoelasticity]

25. Errapart, A. (2008). On the technology of photoelastic tomography, *Experimental Techniques*, 32, 1, 31-35.[New frontier of photoelasticity]

Biographical Sketch

José L.F. Freire: B.S. (1972) and M.Sc. (1975) degrees in mechanical engineering from the Catholic University of Rio de Janeiro (PUC-Rio); Ph.D. (1979) in Engineering Mechanics from Iowa State University of Science and Technology (ISU); associate professor of Mechanical Engineering at PUC-Rio and chairman of the Structural Integrity Laboratory; member of the Society for Experimental Mechanics and its past president; major areas of research: Experimental Stress Analysis, Pipeline Engineering and Structural Integrity of Equipments and Structures.